

Merger Induced Globular Cluster Formation and Galaxy Evolution

F.D.A. Hartwick

*Department of Physics and Astronomy,
University of Victoria, Victoria, BC, Canada, V8W 3P6*

ABSTRACT

Based on the earlier work of Gunn and McCrea we model the formation of globular clusters in merging galaxies. Neutral hydrogen observations of dwarf irregular galaxies as well as more luminous systems are used to provide the key parameters of the model. The observations indicate that clusters with the mass of globular clusters should still be forming today. The model is incorporated into a phenomenological picture of galaxy evolution making use of a simple chemical evolution model. These results are compared to recent observations of the metallicity distributions of F and G stars from a recent large SDSS survey. The comparisons are consistent with an anisotropic collapse and merging of a large number of dwarf irregular galaxies for the formation of the Galaxy.

Subject headings: Galaxy: evolution — Galaxy: halo — globular clusters: general

1. Introduction

One of the remarkable observational facts about the stellar content of galaxies is the ubiquity of globular star clusters. These clusters can be found in almost all but the least massive galaxies. Generally globular clusters come in two major families of comparable mass: metal poor, old blue clusters and metal richer, younger, red clusters. A comprehensive review of globular cluster systems is given by Harris (2001). Below we present quantitative arguments for the formation of clusters during mergers and use the observations to obtain the key parameters of the model. This formation picture leads naturally to a phenomenological model for galaxy evolution. Combined with a simple chemical evolution model comparisons with recent data for Galactic halo stars are made.

2. Merger Induced Globular Cluster Formation

The possibility of forming globular clusters from collisions between gas rich bodies was considered by Gunn (1980) and independently by McCrea (1982). We revive and extend the Gunn and McCrea analysis here.

2.1. The model

Within each of two equal mass interacting galaxies consider an undisturbed column of gas of length l , cross-sectional area A and density ρ_o meeting its counter- part with relative velocity $2V$ (see Fig.1). During the collision, the gas is compressed to column length λ and density ρ . The shocked gas is assumed to cool to $T \sim 10^4$ degrees. This assumption will be justified later-suffice it to say that the cooling time within the compressed volume (τ_{cool}) must be shorter than the collision time ($\tau_{coll} \sim l/V$) for the assumption to be valid. By conservation of mass and for simplicity assuming A to remain constant

$$2\rho_o l A = \rho \lambda A \quad (1)$$

equivalently in terms of the column density

$$2\Sigma_o = \Sigma \quad (2)$$

and

$$\frac{\rho}{\rho_o} = \frac{2l}{\lambda} \quad (3)$$

with the relative velocity being $2V$, the relation between ρ_o and ρ becomes (e.g. Spitzer (1978), equation 10-24)

$$\rho_o 4V^2 \simeq \rho \left(\frac{kT}{\mu m_H} \right) \quad (4)$$

so that

$$\frac{\rho}{\rho_o} \simeq 0.048 V^2 / (T_4 / \mu) \quad (5)$$

where the bracketed quantity in equation (4) represents the square of the sound speed, and in equation (5) the unit of V is km/sec, T_4 is the temperature in units of 10^4 degrees and μ is the mean molecular weight of the shocked gas. The quantity (T_4/μ) occurs frequently in the expressions below. With $\mu = 0.59$ a typical value for this quantity is ~ 1.7 . Combining (3) and (5)

$$\frac{l}{\lambda} \simeq 0.024 V^2 / (T_4 / \mu) \quad (6)$$

The Jean’s length, λ_J is

$$\lambda_J = \left(\frac{\pi k T}{\mu m_H G \rho} \right)^{1/2} \simeq \frac{246}{\rho^{1/2}} (T_4/\mu)^{1/2} \text{ pc} \quad (7)$$

with ρ in units of M_\odot/pc^3 . Equating λ with λ_J eliminating ρ

$$\lambda = \lambda_J = \frac{6.05 \times 10^4}{2\Sigma_o} (T_4/\mu) \text{ pc} \quad (8)$$

Finally, the Jean’s mass is given by

$$M_J = \rho \lambda^3 = 2\Sigma_o \lambda^2 = 6.05 \times 10^4 \lambda (T_4/\mu) M_\odot \quad (9)$$

If the cooling time of this gravitationally unstable mass, τ_{cool} , is shorter than the free-fall time (τ_{ff}) then fragmentation can occur. The cooling function $\Lambda(Z)$ which when multiplied by the square of the particle density of hydrogen gives the cooling rate per unit volume, falls precipitously from a metallicity independent peak near $T \sim T_4$ to a metallicity dependent plateau below (e.g. Dalgarno & McCray 1972). The cooling rate from heavy elements alone at $T_4 \sim 0.9$ is $\gtrsim 4 \times 10^{-26} (Z/Z_\odot) n_H^2$ (e.g. Fall & Rees 1985, §IV, p. 22). From $\tau_{cool} = 1.5nkT/(\Lambda n_H^2)$ and with the density in $M_\odot \text{ pc}^{-3}$ the cooling time scale becomes $\sim 6.96 \times 10^4 (Z/Z_\odot)^{-1} (T_4/\mu)/\rho$ yrs. Similarly $\tau_{ff} = (32G\rho/3\pi)^{-1/2}$ reduces to $\sim 8.08 \times 10^6/\rho^{1/2}$ yrs. Finally, from (3) and (4) one can write $\tau_{coll} = \tau_s \mathfrak{R}$ where $\tau_s = \lambda/c_s \sim 1.07 \times 10^5 \lambda (T_4/\mu)^{-1/2}$ yrs, c_s is the sound speed, λ is in pc, and \mathfrak{R} is the Mach number ($2V/c_s$) and is $\gg 1$. Eliminating the density using (7) the relevant time scale ratios become

$$\tau_{cool}/\tau_{coll} < \tau_{cool}/\tau_s \sim 1.07 \times 10^{-5} \lambda (Z/Z_\odot)^{-1} (T_4/\mu)^{1/2} \quad (10)$$

and

$$\tau_{cool}/\tau_{ff} \sim 3.5 \times 10^{-5} \lambda (Z/Z_\odot)^{-1} (T_4/\mu)^{1/2} \quad (11)$$

As will be shown in the next section, the observationally determined value of λ is such that both of these ratios are less than unity. Hence our assumption that the shock is isothermal is justified. We are also assuming that the temperature of the gas remains constant at the maximum of the cooling function near $T_4 \sim 1$ until the mass becomes Jeans unstable. Further, one can expect fragmentation to occur when the gravitationally unstable cloud begins to collapse as long as Z/Z_\odot is not much less than ~ 0.01 . This is also the threshold metallicity below which globular clusters are not observed.

Assuming that stars are eventually formed, another consideration is the efficiency η with which gas is turned into stars. This is not well known at present so for the later discussion we assume this quantity to be $\eta \sim \Omega_{star}/\Omega_{baryon} \sim 0.07$. This ratio represents the global stellar

mass density divided by the total baryon density. A further question then arises because the mass loss associated with star formation and evolution can lead to the dissolution of any cluster of stars formed. This problem has been investigated by Geyer & Burkert (2001) and more recently in their discussion of the globular cluster mass function by Parmentier & Gilmore (2007). Unfortunately the observations which would allow an empirical estimate of the bound to unbound stellar ratio are not yet available so that more sophisticated modelling is required to answer this question in the context here. To proceed we shall consider η to set an upper limit to the mass of a bound cluster of stars formed.

A final point to note is that in this model the gas is concentrated by collision and the co-orbiting stars and dark matter will at least initially be unaffected by this process. Hence we do not expect the resulting globular clusters to contain a significant amount of dark matter.

2.2. Relating the model to the Observations

It is clear from the above discussion that the crucial quantity to determine is λ while the principal variables are a characteristic length l , and a characteristic velocity V . Given that the available observational parameters of the dominant gaseous component of galaxies are the radius of the HI disk, r_{HI} , the mass of the HI gas, M_{HI} , and the peak rotational velocity of the HI, V_{rot} , we begin by identifying l with r_{HI} and V with V_{rot} . By identifying V with V_{rot} we are considering mainly edge-on collisions. While the mass does not directly enter into the discussion above, correlations between it and the other variables lead to interesting results. The mass parameter actually used here is $1.3M_{HI}$ in order to allow for the contribution of helium. Throughout the rest of this work, the symbol M_{HI} will generally represent both the hydrogen *and* helium gas content.

The data discussed here comes from two sources. The first for relatively bright galaxies are from Broeils and Rhee (1997) and the second for dwarf irregular galaxies are from Begum et al.(2008a,b). In order to intercompare both data sets a correction to both r and M was made for the small difference in assumed Hubble constant. In addition because the HI radii were measured at a different limiting surface brightness, a correction of $+0.178$ in $\log r$ was applied to the Broeils and Rhee data. This was determined by jointly correlating the radii and the masses and finding the minimum dispersion. This correction is well within the uncertainties quoted by Begum et al. in their discussion of this problem. Fig. 2 shows the resulting relation between $2 \log r_{HI}$ and $\log M_{HI}$. The solid line has a slope of 1 while a least squares fit for this slope gives 0.994 ± 0.012 for all 137 galaxies. The logarithmic intercept ($\log M - 2 \log r$) is 0.846 ± 0.132 . Hence in agreement with Begum et al. the HI surface

density appears to be remarkably constant over nearly 5 orders of magnitude in mass. Note that this face-on surface density is not to be confused with Σ_o above where it represents the column density.

Equation (6) above implies that if λ is a constant then a relation between $2 \log V$ and $\log r$ should determine its value. Fig.3 shows such a plot. Possibly a more familiar way to look at this relation is to eliminate r by using the relationship established in Fig.2. Since $r \propto M^{1/2}$ equation (6) implies $M \propto V_{rot}^4$ i.e. an HI Tully-Fisher relation is predicted. This is shown in Fig.4. The solid line in both Figs 3 & 4 has a slope of 1. Least squares fit to the data with $V_{rot} > 41.7 \text{ km s}^{-1}$ (i.e. above the dashed lines) give 0.978 ± 0.078 in Fig.3 and 0.989 ± 0.089 in Fig. 4. Both regressions included 109 galaxies. The logarithmic intercepts are $(\log r - 2 \log V_{rot}) = 0.168 \pm 0.250$ and $(\log M - 4 \log V) = 1.18 \pm 0.515$. Solving for λ from each one obtains $\lambda = 61.3 \pm 35.3(T_4/\mu) \text{ pc}$ and $\lambda = 61.4 \pm 36.3(T_4/\mu) \text{ pc}$ respectively. Although the uncertainties are large the numerical difference is small given the tight correlation seen in Fig. 2. Given this value of λ the time scale arguments above are justified. It should be noted however that the condition for fragmentation will be violated for values of Z/Z_\odot not much below 0.01. This provides a natural explanation for the observed abundance threshold of this order below which globular clusters are not observed a point also made by Gunn (1980).

Returning to equation (9) the Jean's mass becomes $M_J = 3.7 \pm 2.1 \times 10^6 (T_4/\mu)^2 M_\odot$. Allowing for a gas to star formation efficiency of $\eta \sim 0.07$ results in a predicted globular cluster mass upper limit of $M_{GC} \sim 2.6 \pm 1.5 \times 10^5 (T_4/\mu)^2 M_\odot$.

Begum et al. (2008a) have also noted that the dwarf irregular galaxies with the lowest rotational velocities (i.e. those below the dashed line in Figs 3 & 4) lie below the extrapolated baryonic Tully-Fisher relation. If all of the galaxies are rotationally supported, then $V_{rot}^2 = \alpha G M_{HI} / r_{HI}$ where α is the ratio of the total mass enclosed within r_{HI} to the gas mass. Given the relatively tight relation in Fig.2 the increased scatter in Figs 3 & 4 can be understood as due to variations in this ratio. In order to account for the data below the dashed lines, either the gas is not fully rotationally supported or there is a systematic shift in the value of α towards a lower value inspite of the tight correlation between the HI radius and mass in fig. 2.

Suppose that the galaxies below the dashed lines are indeed relatively gas rich (i.e. low α). These objects could then be more representative of the universe as it was 13 Gyr ago and be the proto-galactic clumps from which the present galaxies were assembled. Fitting lines of slope unity through these 28 points in figs 3 and 4 then yields values of λ of $310 \pm 272(T_4/\mu) \text{ pc}$ and $307 \pm 271(T_4/\mu) \text{ pc}$ respectively i.e. a factor of ~ 5 higher than from the more massive galaxies and hence a Jean's mass higher by the same amount.

In order to recover the observed globular cluster masses one would need to invoke a star formation efficiency smaller by the same amount. In any event because the clusters are old and relatively metal poor, it will be argued below that these clusters were formed from the mergers of dwarf irregular galaxies whether those below the dashed lines in figs 3 and 4 or at the low mass end of those above.

At the beginning of this discussion we chose to identify the l and V of the model with r_{HI} and V_{rot} of the gas rich galaxies. The choice of V_{rot} would seem to be natural since during the interaction between two counter rotating galaxies the undisturbed gas is rotationally supported. The choice of r_{HI} for l then leads to a ‘reasonable’ mass for a globular cluster. A further consistency check comes from the model prediction that the column density of gas ($\Sigma_o = \rho_o l$) must be a constant and equal to $\Sigma_o = 3.02 \times 10^4 (T_4/\mu)/\lambda$. With the value of λ derived above (assuming $l=r_{HI}$) $\Sigma_o = 496 \pm 285 M_\odot pc^{-2}$. This in turn implies a value for the undisturbed particle density varying from $\sim 7 - 0.2$ gas particles/cm³ as the galaxy radius increases from 2.5 to 100 kpc. For a Milky Way sized galaxy, ($r_{HI} \sim 25$ kpc), $n_H \sim 0.6 \pm 0.4 cm^{-3}$ compared to an observed value of $n_H = 0.57 cm^{-3}$ (Dickey & Lockman 1990).

If structure in the universe forms hierarchically as is currently believed i.e. low mass structures form first and merge to make larger objects, then we expect the oldest clusters to have been formed at the time when the low mass systems were merging. In fact genuine globular clusters (both blue and red) are found in many ‘surviving’ dwarf irregular galaxies (e.g. van den Bergh 2006, Georgiev et al. 2008). Generally, as larger structures merge, we expect clusters of similar mass to form but have progressively younger ages and higher metallicities. Today, given the right circumstances, these objects should still be forming and may resemble the super star clusters first observed by Schweizer (1987) in the Antennae galaxies. Conversely, the Galactic building blocks could not have been much more massive than the dwarf irregular galaxies before merging or the red globular cluster backbone would have been younger and more metal rich than observed.

In the next section an outline of galaxy formation based on this picture is presented.

3. Implications for Galaxy Evolution

We now incorporate the above cluster formation model into an outline for galaxy evolution. The two separate globular cluster families (i.e. the old metal poor blue ones and the slightly younger metal rich red ones) are also found in different locations in a galaxy. Unlike the red clusters which are almost exclusively found in the inner regions of galaxy halos,

the blue globular clusters can be found in both the inner and outer regions (e.g. Harris, 2001). In order to account for these differences we invoke an anisotropic collapse picture. We imagine that a spiral galaxy forms within a filament of proto-galactic clumps of gas and dark matter. The filament is assumed to collapse first in a direction perpendicular to the filament length and then along its length. Generally the angular momentum content of a galaxy is distributed so we expect the low angular momentum building blocks to collide in the first collapse and in a major burst of star formation form the blue clusters and associated field stars. While the previously formed stars and dark matter will form a more diffuse background, the gas left over after the star formation burst from which the blue globulars and associated field stars form will fall to the center and eventually be available to form the nucleus of the galaxy and contribute to the low angular momentum component of the bulge. The end result is a population of field stars formed prior to the mergers and their associated dark matter halos and post-merger blue globulars and stars formed as a result of the merging activity but with different kinematics than the prior population. The higher angular momentum building blocks continue to become enriched and slowly spiral in towards the center at which time they begin colliding with each other and leave behind a diffuse background of stars, dark matter and any previously formed blue globular clusters. The gas undergoes a second major burst of star formation and red globular cluster formation before the residual gas eventually falls to form the disk. A chemical evolutionary model based on this picture which was also able to account for the global star formation history was given in H04. Here we compare the model to new and previously unavailable data based on a large survey of stars with photometric metallicity determinations from the Sloan Digital Sky Survey (Ivezic et al. 2008).

Before discussing the observations we shall describe the chemical evolution model used to make the comparisons. It is similar to the model described in H04. There the equations are modified slightly from a one zone mass loss model in order to mimic a multi-zone model which works as follows. Suppose that in the one zone model the chemical evolution is interrupted before all of the gas has turned into stars as might occur during a merger for example. We are then left with a sharply truncated metallicity distribution of stars and a mass of gas with a single metallicity. Now suppose that these truncations occur over a finite range of metallicity dictated by a Gaussian distribution for example. Then we shall end up with a more smoothly truncated stellar distribution and finite spread in the metallicity of the left over gas which should be almost Gaussian shaped. The end result mimics the result of many zones having undergone truncations (mergers) over a range of metallicity. The model also allows for mass loss to occur at a rate proportional to the star formation rate by defining an effective yield.

Fig. 5 is taken from the paper of Ivezic et al. (2008) (bottom right of their fig. 7).

The points with error bars show the metallicity distribution of halo stars with height above the plane $|Z| = 5-7$ kpc. The blue curve shows the predicted metallicity distribution of the left over gas after the collisions have taken place. Because the model does not predict either the metallicity distribution or the mass of the stars formed during the mergers we have assumed that the post-merger stellar and cluster distribution is the same as that of the left over gas and used a gas to star formation efficiency of ~ 0.07 to estimate the mass of the stars and clusters. The solid black line (arbitrary normalization) shows the distribution of metallicity of the stars formed prior to the mergers. It was calculated using exactly the same chemical evolution model given in H04. The model parameters are $\log(p_{eff}/Z_{\odot}) = -0.3$, $\log(Z_c/Z_{\odot}) = -1.50$, and $\sigma_{blue} = 0.32$. Using the above star formation efficiency, the ratio of the mass of stars formed during the mergers to those formed prior to the collisions is ~ 0.8 . This number will also depend on the value assumed for p_{eff} . For illustrative purposes here and to minimize parameters we have kept the effective yield the same as the true yield (i.e. $0.5Z_{\odot}$). The stars formed prior to the merger are clearly more metal poor than the post-merger population and apparently do not show up in the data in Fig. 5 although no attempt was made to fit more than one component to the data. These stars are expected to have different kinematic properties since they would not have been affected in the same way by the collisions which produced the burst of star formation and clusters. In fact, these stars may belong to the second blue halo population which is more metal poor and with different kinematics identified in a deeper survey by Carollo et al. (2007).

Note that a prediction of this model is that generally the stars enclosed by the blue curve should have the same kinematics and spatial distribution as the blue (halo) globular clusters since they are assumed to have formed at the same time. Further these clusters should belong to the ‘young’ halo group of Zinn (1993).

Fig. 6 from the top right of fig 7 of Ivezić et al. shows a similar plot but now with stars from $|Z| = 1.5 - 2.0$ kpc. Here the red curve is the chemical model metallicity prediction assumed for stars and red clusters formed during the second set of collisions. Instead of using a Gaussian to determine the metallicity distribution of the stars/clusters formed during the collisions, we have used an extreme value distribution function which has the shape of an asymmetrical Gaussian. i.e. the function f of H04 is replaced by

$$f = \exp(-\exp(-(\log Z_c - \log Z)/w)) \quad (12)$$

and the Gaussian function in equation (8) of H04 ($df/d\log Z$) is replaced by the expression

$$df/d\log Z = \exp((-(\log Z_c - \log Z)/w) - \exp(-(\log Z_c - \log Z)/w))/w \quad (13)$$

The model parameters are $\log(p_{eff}/Z_{\odot}) = -0.3$, $\log(Z_c/Z_{\odot}) = -0.68$, and $w = 0.16$. This function could have been used for the blue clusters as well but the fit was marginally better using the Gaussian for them given that only one component was being fit.

The solid black line (arbitrary normalization) shows the metallicity distribution of all stars formed in the surviving population of building blocks prior to the second major merger phase. This group of stars (called the red spheroid in H04) will be more diffuse, have different kinematics and will possess a metal weak tail. The mass ratio between these two components (post to prior) for the parameters assumed above is ~ 0.2 .

Note that any blue clusters that formed prior to the first major merger phase and which remained bound to its lower mass galaxy while avoiding the first mergers will also have the kinematics of the red spheroid population and hence would be members of the ‘old’ halo component of Zinn (1993). The red clusters should have the same kinematics as the stars under the red curve of fig 6. The closest analog of a thick disk population in this model are these same stars.

The main purpose of this discussion is to show that the phenomenological model outlined above is at least qualitatively consistent with the new data and with our picture of globular cluster formation. Further, the general outline for galaxy evolution described above may help explain additional globular cluster related questions. For example, the blue-red cluster phenomenon is also present in elliptical galaxies even though they are morphologically quite different from the gas rich systems. Could it be that ellipticals formed similarly but at the intersection of more than one filament? The increased frequency of collisions would convert more gas to stars and lead to a higher specific frequency of globular clusters. In both cases variations in the distribution of angular momentum content could explain the differences in the relative frequency of blue to red clusters. We leave these interesting questions to future work.

4. Conclusions

We have given a quantitative model for the formation of globular clusters based on the early work of Gunn & McCrea. Clusters are assumed to form in merger induced collisions. We make use of recent HI data for dwarf irregular galaxies and earlier observational work to derive the key parameters of the model. We then combined this model with a simple chemical evolutionary model to predict the metallicity distributions of stars formed before and during these mergers. These predictions were compared with relatively recent survey data and shown to be consistent with both models. As additional data becomes available it will be possible to refine these ideas into a more sophisticated picture for galaxy evolution.

The author is grateful to Zeljko Ivezic for promptly sending the data contained in Fig. 7 of their important paper. He also wishes to thank Brent Tully for suggesting references to

the literature, Ray Carlberg for helpful comments and the referee for a constructive report.

REFERENCES

- Begum, Ayesha, Chengalur, Jayaram N., Karachentsev, I. D., & Sharina, M. E. 2008a, MNRAS, 386, 138
- Begum, Ayesha, Chengalur, Jayaram N., Karachentsev, I. D., Sharina, M. E., & Kaisin, S. S. 2008b, MNRAS, 386, 1667
- Broeils, A.H. & Rhee, M.-H. 1997, A&A, 324,877
- Carollo, Daniela; Beers, Timothy C.; Lee, Young Sun; Chiba, Masashi; Norris, John E.; Wilhelm, Ronald; Sivarani, Thirupathi; Marsteller, Brian; Munn, Jeffrey A.; Bailer-Jones, Coryn A. L.; and 2 coauthors 2007, Nature, 450, 1020
- Dalgarno, A. & McCray, R.A. 1972, ARA&A, 10, 375
- Dickey, J. M. & Lockman, F. J. 1990, ARA&A, 28, 215
- Fall, S. M. & Rees, M. J. 1985, ApJ, 298, 18
- Georgiev, Iskren Y., Goudfrooij, Paul, Puzia, Thomas H., & Hilker, Michael 2008, AJ, 135, 1858
- Geyer, M. P. & Burkert, A. 2001, MNRAS, 323, 988
- Gunn, J. E. 1980, in Globular Clusters, ed. D. Hanes and B. Madore (Cambridge: University Press) p.301
- Harris, W. E. 2001, in Star Clusters, ed. L. Labhardt & B. Binggeli (Berlin: Springer) p. 223
- Hartwick, F.D.A. 2004, ApJ, 603, 108 (H04)
- Ivezic, Zeljko; Sesar, Branimir; Juric, Mario; Bond, Nicholas; Dalcanton, Julianne; Rockosi, Constance M.; Yanny, Brian; Newberg, Heidi J.; Beers, Timothy C.; Allende Prieto, Carlos; and 43 coauthors 2008, ApJ, 684, 287
- McCrea, W.H. 1982, in Progress in Cosmology, ed. A. W. Wolfendale (Dordrecht, Reidel) p. 239
- Parmentier, G. & Gilmore, G. 2007, MNRAS, 377, 352
- Schweizer, F. 1987, in Nearly Normal Galaxies: From the Planck Time to the Present, ed. S.M. Faber (Berlin: Springer), 18
- Spitzer, L. 1978, Physical Processes in the Interstellar Medium (New York, Wiley) p. 221

van den Bergh, S. 2006, *AJ*, 131, 304

Zinn, R. 1993, in *Globular Clusters-Galaxy Connection*, ed. G. H. Smith & J. P. Brodie
(San Francisco: ASP), 38

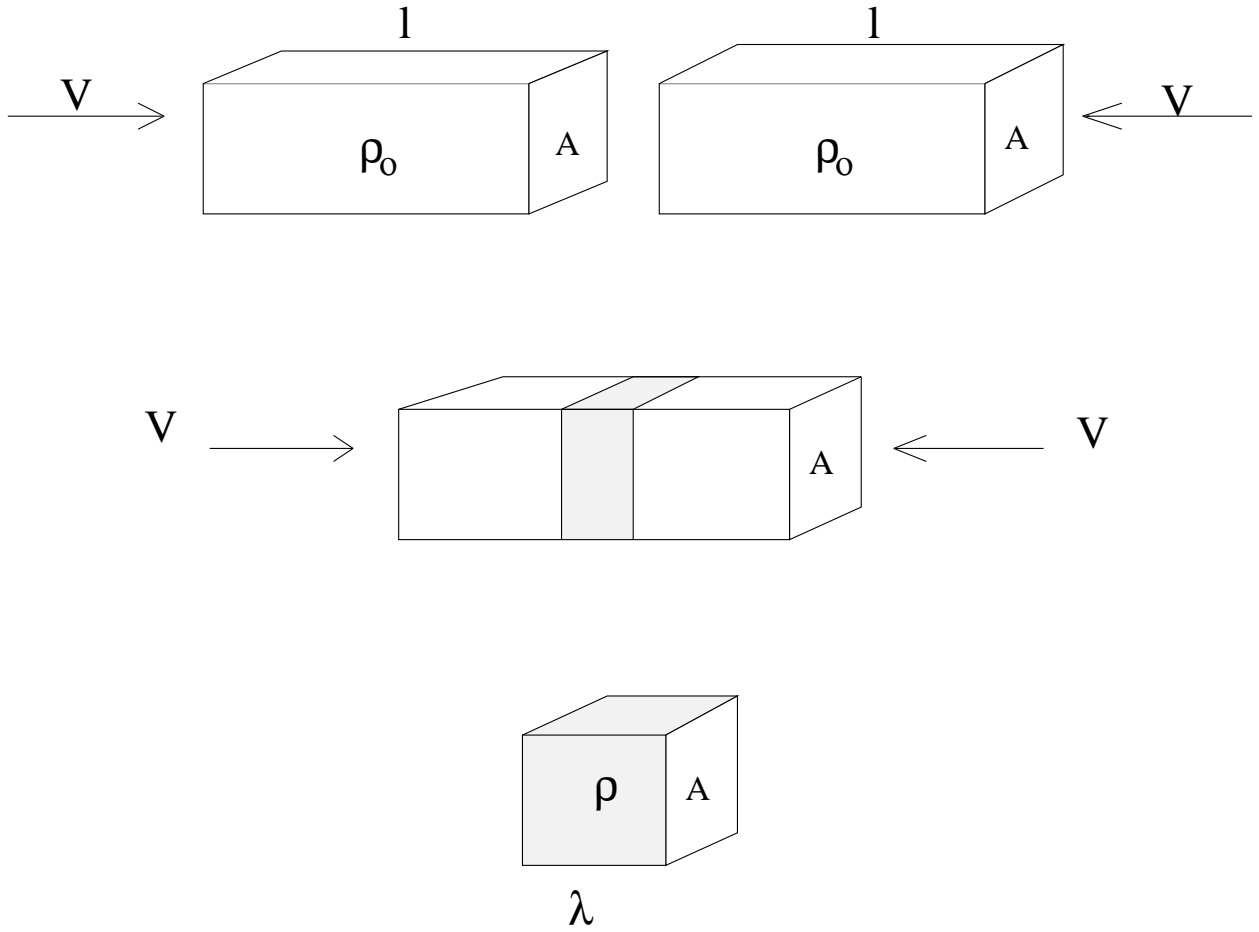


Fig. 1.— Two gas columns approach one another with relative velocity $2V$ and collide reducing the column length from l to λ and increasing the density from ρ_0 to ρ

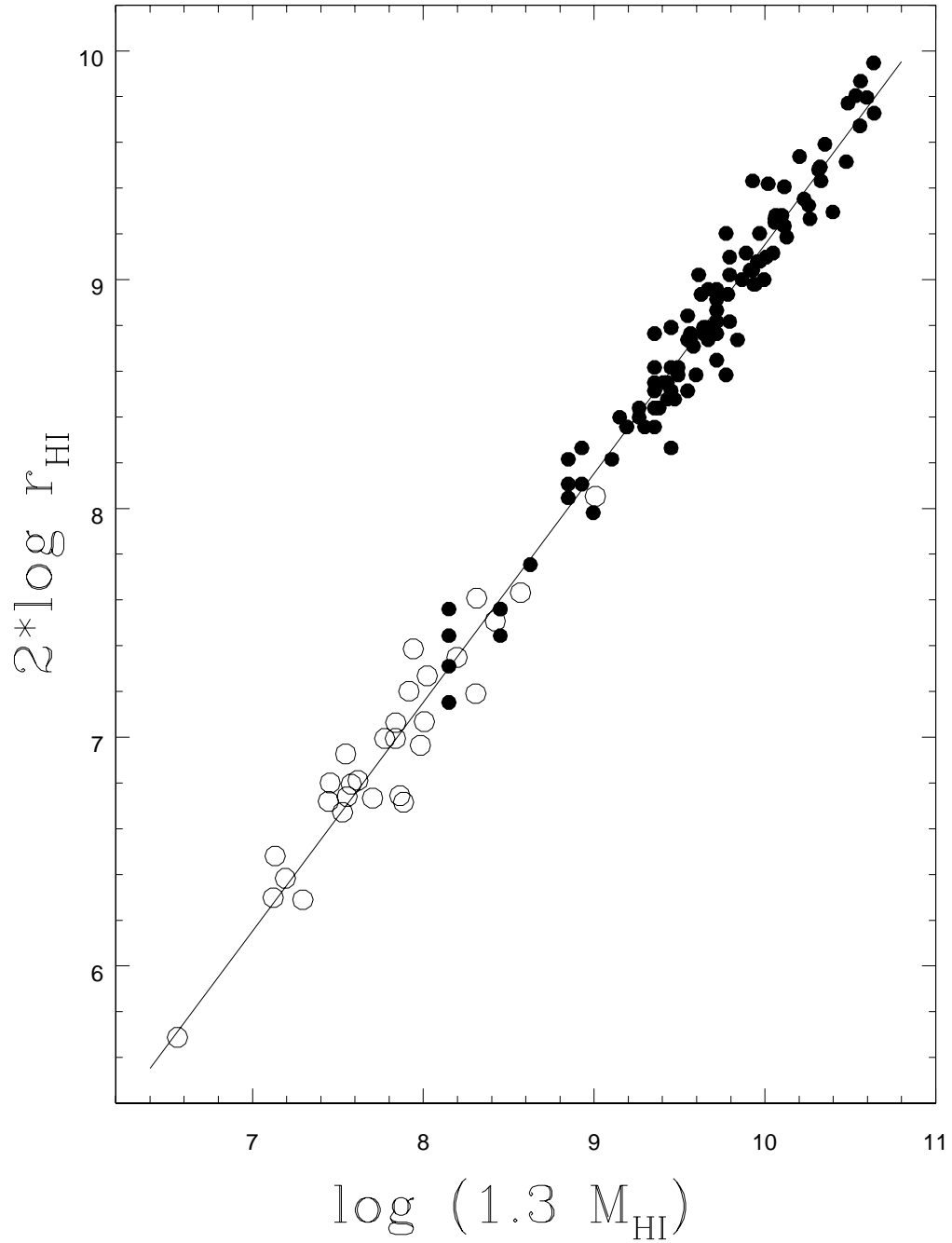


Fig. 2.— Twice the log of the radial extent of the neutral hydrogen gas r_{HI} versus the log of $1.3 \times M_{HI}$. The solid line has a slope of unity. The solid points are from Broeils & Rhee (1997) while the open circles are from the work of Begum et al. (2008a,b). The units of r_{HI} and M_{HI} are pc and M_{\odot} respectively.

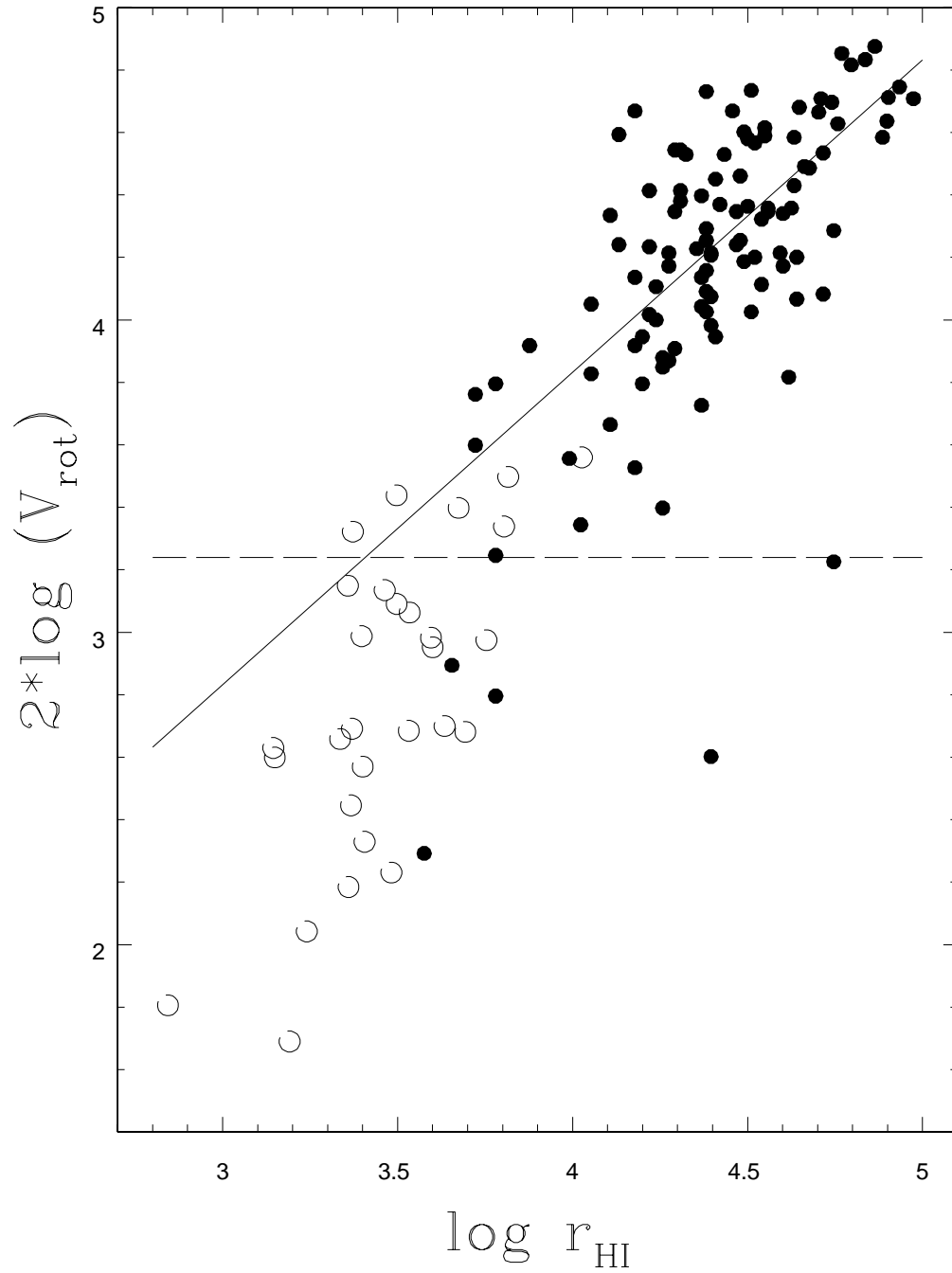


Fig. 3.— Twice the log of the rotation velocity of the neutral hydrogen versus the log of its radial extent. The solid line has a slope of unity and the dashed line is the adopted lower limit of the velocity below which the predicted relation is assumed to break down. The symbols are as defined in fig. 2. The unit of rotational velocity is km/sec

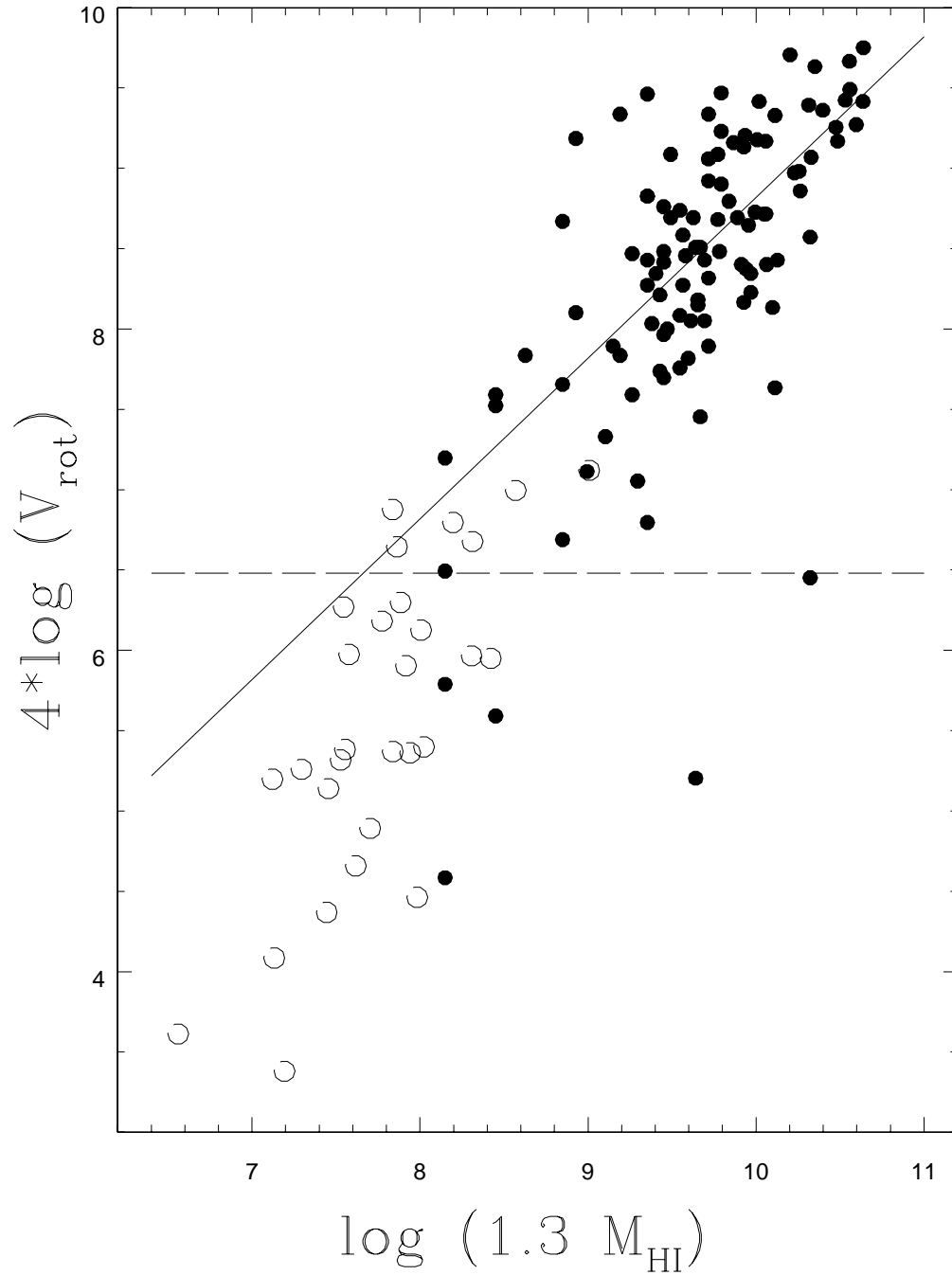


Fig. 4.— Four times the log of the rotation velocity versus the log of the mass of gas. The solid line has a slope of unity and the dashed line is the adopted lower limit to the velocities of galaxies assumed to be obeying the HI Tully-Fisher relation. The symbols are as defined in fig.2.

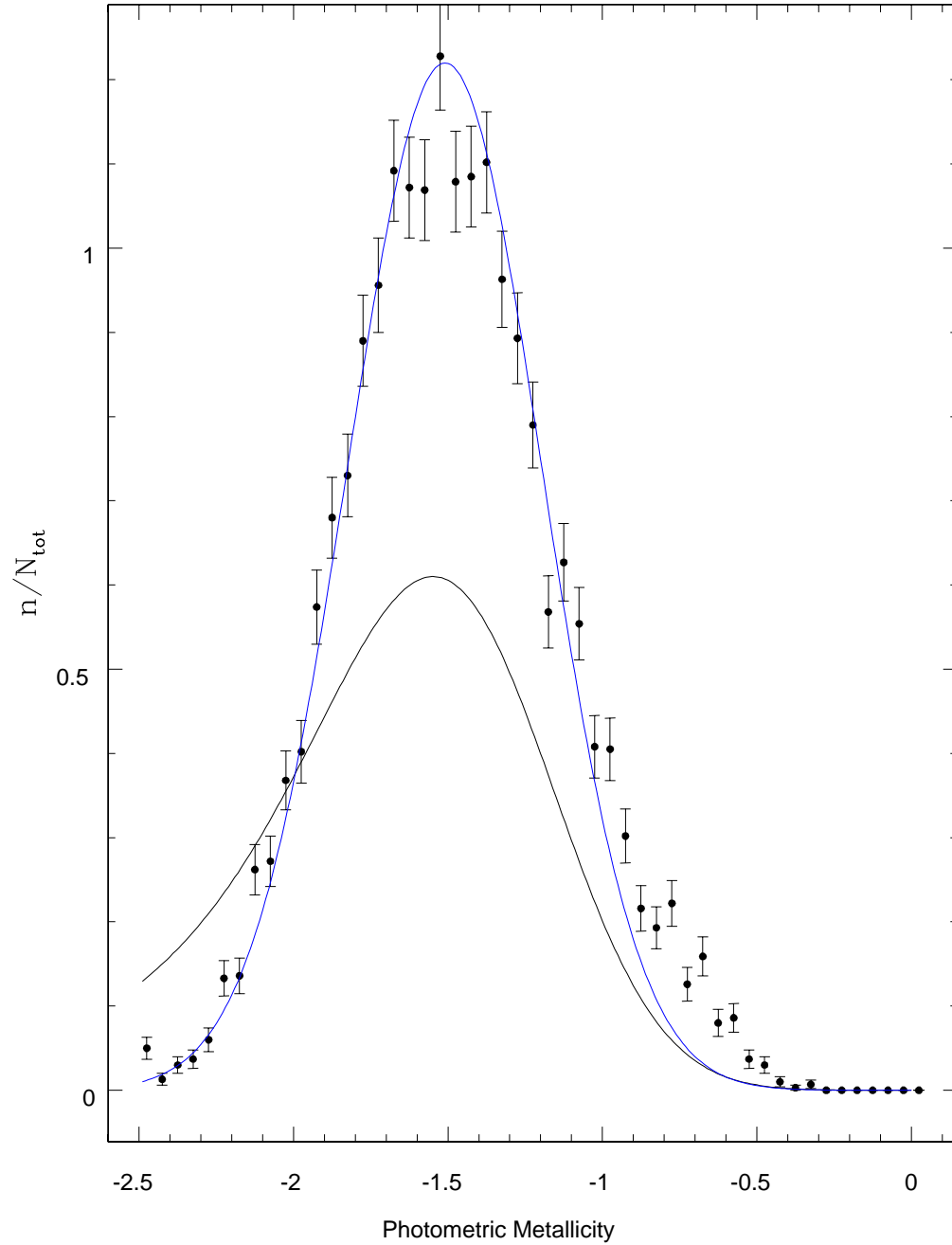


Fig. 5.— The data points are from fig 7 (bottom right) of Ivezić et al. (2008) and show the metallicity distribution of stars within the distance interval above the plane of $|Z| = 5 - 7$ kpc. The blue line is derived from the chemical evolution model under the assumption that the stars were formed in a major merger phase associated with the formation of the blue globular clusters. The black line shows the predicted distribution of metallicities of the stars which formed prior to the merger phase. The normalization of this curve is arbitrary.

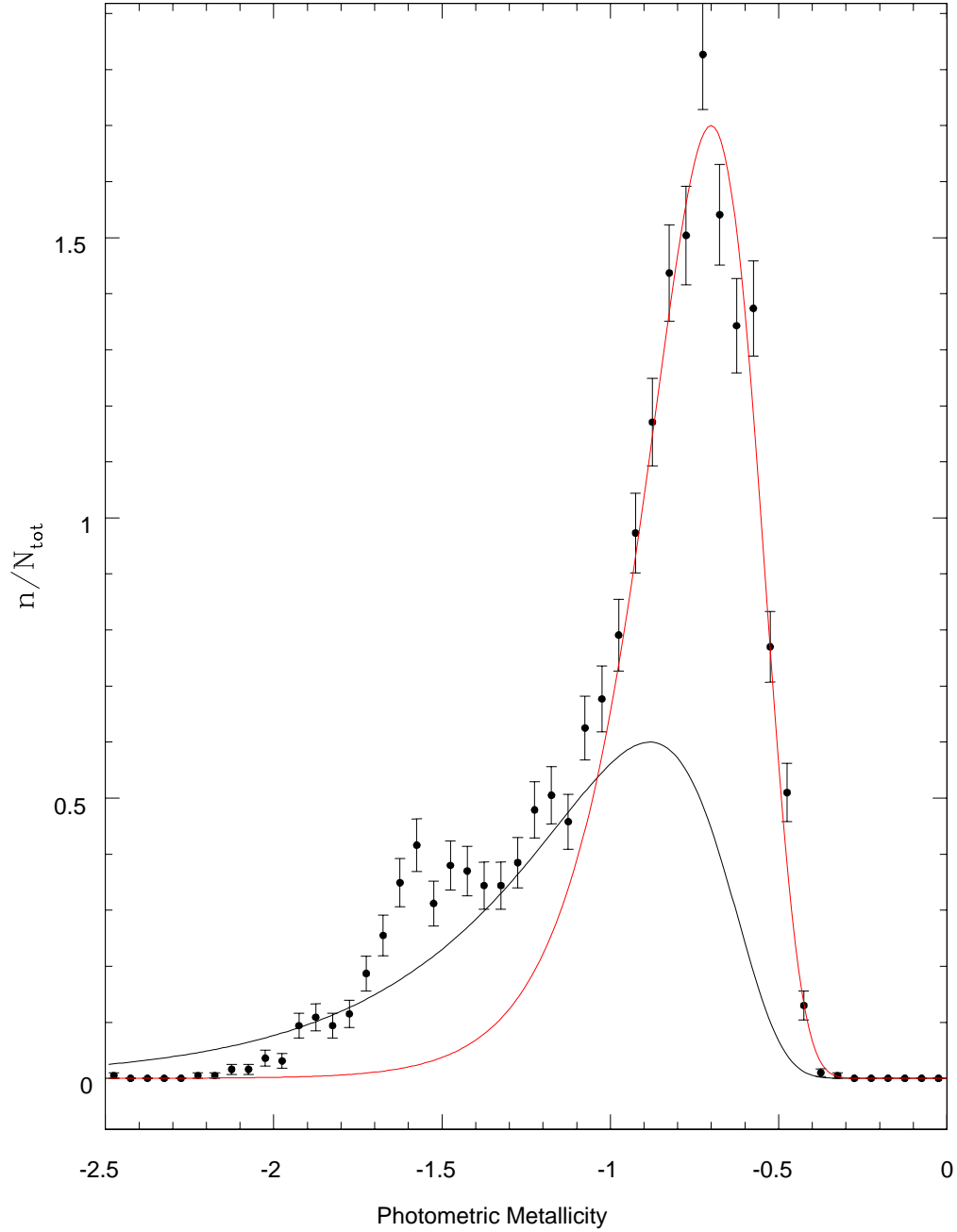


Fig. 6.— The data points are from fig 7 (top right) of Ivezić et al. (2008) and show the metallicity distribution of stars within the distance interval above the plane of $|Z| = 1.5 - 2.0$ kpc. The red line is derived from the chemical evolution model under the assumption that the stars were formed in a second major merger phase associated with the formation of the red globular clusters. As above the black line with arbitrary normalization shows the predicted distribution of metallicities of stars formed prior to the mergers.